Received February 5, 2021, accepted March 3, 2021, date of publication March 10, 2021, date of current version March 18, 2021.

Digital Object Identifier 10.1109/ACCESS.2021.3065400

A Secured Social-Economic Framework Based on PEM-Blockchain for Optimal Scheduling of Reconfigurable Interconnected Microgrids

FENGYUAN YIN[1], ALI HAJJIAH[2], KITTISAK JERMSITTIPARSERT[3,4], AMEENA SAAD AL-SUMAITI[5], (Senior Member, IEEE), SALAH K. ELSAYED[6], SHERIF S. M. GHONEIM[6], (Senior Member, IEEE), AND MOHAMED A. MOHAMED[7,8], (Member, IEEE)

[1]Department of Mechanical and Electrical Engineering, Wuhan Qingchuan University, Wuhan 430204, China
[2]Electrical Engineering Department, College of Engineering and Petroleum, Kuwait University, Safat 13060, Kuwait
[3]Faculty of Administrative, Economic and Social Sciences, University of City Island, Gazimağusa 99450, Northern Cyprus
[4]Faculty of Social and Political Sciences, Universitas Muhammadiyah Sinjai, Sulawesi Selatan 92615, Indonesia
[5]Advanced Power and Energy Center, Electrical Engineering and Computer Science Department, Khalifa University, Abu Dhabi, United Arab Emirates
[6]Department of Electrical Engineering, College of Engineering, Taif University, Taif 21944, Saudi Arabia
[7]Electrical Engineering Department, Faculty of Engineering, Minia University, Minia 61519, Egypt
[8]Department of Electrical Engineering, Fuzhou University, Fuzhou 350116, China

Corresponding authors: Kittisak Jermsittiparsert (kittisak.jermsittiparsert@adakent.edu.tr), Ameena Saad Al-Sumaiti (ameena.alsumaiti@ku.ac.ae), and Mohamed A. Mohamed (dr.mohamed.abdelaziz@mu.edu.eg)

This work was supported in part by the Taif University Researchers Supporting Project, Taif University, Taif, Saudi Arabia, under Grant TURSP-2020/34.

ABSTRACT Optimal scheduling of reconfigurable interconnected microgrids is a precious and critical task for the residential consumers especially with the integration of renewable energy sources, dispatchable units and energy storage systems. In this regard, not only the optimal scheduling of the microgrids in a realistic and correlated environment is a necessity, but also the guarantied security and the prevention of cyber-attacks are mandatory tasks for the operators. This article first addresses these issues by developing a novel framework based on blockchain for secured data transaction from the individual microgrids' components to the central control unit and then tries to find the optimal scheduling plan using stochastic programming based on point estimate method (PEM). Through such a hybrid PEM-blockchain based framework, the interconnected microgrids can supply the residential loads in a fully reliable, economic and secured structure. We also consider a social-economic framework to not only minimize the total operating cost of the microgrids, but also benefit the customers by enhancing the social factors through the optimal switching. Considering the complex and nonlinear nature of the problem, an effective corrected crow search (CCS) algorithm is deployed to find the most optimal operating point for the microgrids. The quality and capabilities of the proposed model are investigated using a practical residential interconnected microgrid. The results show that the optimal switching could reduce the total operation cost from \$22,716 to \$21,935 (3.56% reduction). Also, the average energy not supplied (AENS) has reduced from 1.4115 to 1.352 kWh/customer.yr (4.40% reduction), which are notable values. The results advocate the quality and functionality of the proposed framework.

INDEX TERMS Reconfigurable interconnected microgrid, social-economic analysis, blockchain, point estimate method, corrected crow search, stochastic programming.

NOMENCLATURE

A. SETS/INDICES

RCS	Index for controllable switches for reconfiguration
$\_,\overline{\_}$	Lower, upper bounds
Ω^{SW}/sw	Set/index for feeder switches
$\Omega^{DF}/km, mn$	Distribution feeder set/indices
$\Omega^{TF}/km, mn$	Tie feeders set/indices
Ω_i^N/n	Set/index for nodes in i^{th} microgrid ($\Omega_i^{NG} \cup \Omega_i^{NS} \cup \Omega_i^{NAD}$)
Ω_i^{BAD}	Set of buses with adjustable loads in ith microgrid

The associate editor coordinating the review of this manuscript and approving it for publication was Jagdish Chand Bansal.

Ω_i^{NG}	Set of nodes with installed DG in ith microgrid
Ω_i^{NS}	Set of nodes(bus) as well as energy storage in ith microgrid
Ω^{Cus}/j	Electric customers sets/indices
Ω^{MG}/i	Microgrids set/index
Ω^{T}/t	Operation time horizon set/index

B. CONSTANTS

$CT_{i,m}^S, DT_{i,m}^S$	Min charging and discharging times
$E_{i,m}^{AD}$	Total energy required by the adjustable loads
F	Nonlinear function
f_{ul}	PDF of the l^{th} uncertain parameter u
La_j	Average load connected to bus
$\mathrm{N_{branch}}$	Number of branches
$\mathrm{N_{bus}}$	Number of buses
$\mathrm{N_{loop}}$	Number of loops
R_{mn}, X_{mn}, Z_{mn}	Network characteristics including the resistance, reactance, and impedance
$RU_{i,n}^G, RD_{i,n}^G$	Ramp up and down rates for DGs
$UT_{i,n}^{AD}$	Least up time for adjustable load
$UT_{i,n}^G, DT_{i,n}^G$	DG units minimum up and down time
δ	One period of time (1 hour)
$\eta_{i,m}^{Ch}, \eta_{i,m}^{Dch}$	Storage charging/discharging efficiency
$z_{i,n}^G$	Price of (non/) dispatchable unit power generation
z_t^M	Price of electricity market
$\sigma_{i,n}, \omega_{i,n}$	Adjustable loads start/end time
μ_{ul}	Expected value of the uncertain parameter u_l
ρ	Number of uncertain parameters
Δ	Randomization parameter
∂	Constant value

C. VARIABLES

$C_{i,n,t}^S$	Energy stored in the storage
cf_i^{Iter}	Flight length of i^{th} crow in iteration number $Iter$
$I_{mn,t}^F$	Current flow in the feeder
$P_{i,n,t}^{Ch}, P_{i,n,t}^{Dch}$	Amount of charging and discharging
$P_{i,n,t}^D, Q_{i,n,t}^D$	Active and reactive demand
$P_{mn,t}^F, Q_{mn,t}^F$	Feeder active and reactive power flow
$P_{i,n,t}^G, Q_{i,n,t}^G$	Active and reactive power generated by DG
$P_{i,n,t}^M, Q_{i,n,t}^M$	Utility grid active/reactive power
r_i	Random variable in [0,1]
S	Output variable in the stochastic problem
$T_{i,n,t}^{Ch}, T_{i,n,t}^{Dch}$	Successive hours of charging and discharging
$T_{i,n,t}^{G-on}, T_{i,n,t}^{G-off}$	Successive ON and OFF hours for DG
$T_{i,n,t}^{AD-on}$	Successive ON hours for adjustable loads
T_q	Average time used by a node to prepare its block data
T_{sig}	Time elapsed to confirm the signature
$T_{back-off}$	Back-off time associated with the protocol
T_{trm}	Time used for data transfer from a microgrid to other one
t_{prod}	Time used to calculate the data for the block
t_{Mining}	Time of data block
u	Uncertain variable
$V_{i,n,t}$	Bus voltage magnitude
$w_{mn,t}^F$	Status of the feeders
X_i	i^{th} crow in the population
$\alpha_{i,n,t}^G$	ON/OFF state of the DG units
α_j^{Iter}	Best situation which a crow could achieve so far
δ	Grid connected status of the interconnected microgrid
$\vartheta_{l,k}$	Standard location
$\beta_{i,n,t}^{Ch}, \beta_{i,n,t}^{Dch}$	Storage status
$z_{i,n,t}^{AD}$	Status of adjustable loads
$\Delta V_{mn,t}$	Auxiliary voltage variable that is needed to apply KVL
$\theta_{mn,t}^F$	Fictitious current flow of the feeders
$\theta_{i,n,t}^M$	Fictitious current flow of the grid
$\theta_{i,n,t}^D$	Current flow demand for fictitious

I. INTRODUCTION

Microgrid concept is a new and valuable technical term for covering the old concerns of the power researchers in relevance to distributed generations (DGs), renewable energy sources, active networks, storage units and demand response [1]. The benefits associated with the microgrid design and deployment in the power grid are not limited to the lower electricity billing, reinforced reliability and electric power quality, power loss mitigation, operation and planning cost mitigation, clean power production and so on [2]. On the other hand, the high penetration of power storage units such as batteries and renewable energy sources can create new opportunities for more beneficial operation and management of energy among the customers [3]. This is more visible in the interconnected microgrids with the power/energy exchanging capability and self-healing features [4]. In fact, the interconnected microgrids make it possible for the single microgrid to share the extra power generation/storage capacities with each other and thus reduce the costs and improve the power quality [5]. This is also important from the independent system operator (ISO) point of view since it can be used as an effective ancillary service to the main grids [6]. According to the IEEE-1547.4 protocol [7], the idea of breaking down the power grid into several sub-grids can enhance the scalability, efficiency and reliability. It means that this protocol advocates the idea of interconnected microgrids compared to the other types of power delivery at the transmission and distribution scales [8]. Nevertheless, there are new challenges appearing in the interconnected microgrids, especially around

the optimal scheduling [9], how the energy is shared [10], security of data transactions [11] and social and economic preferences [12]. In recent years, several researches have been made to address these issues, which a comprehensive summery is provided in the rest.

In [13], different operation and management schemes are assessed for the interconnected microgrids based on the transactive energy concept. In this regard, the chance-constrained optimization is considered in a stochastic frame for handling the uncertainty effects. Also, the work in [13] attempts to maximize the total benefits of the microgrids by accommodating the combined heat and power idea. In [14], the optimal power management problem is solved for the interconnected microgrids in the market with uncertainty effects. A two-level distributed solution based on cloud-edge and fair pricing is deployed to share the power/energy among the microgrids. The solver is based on the target cascading and augments Lagrange approaches. In [15], the transactive energy concept is deployed for the optimal energy management problem in the interconnected microgrids with a 100% renewable energy sources penetration. In order to mitigate the power variations due to the randomness in power generation from renewable energy systems, hydrogen energy storage is utilized. A stochastic hybrid approach based on fast forward and autoregressive integrated moving average (ARIMA) is devised to meet the effect of the uncertainty in the problem. The authors in [16] have tried to consider each microgrid as an energy hub and thus replace the idea of interconnected microgrids with multi-energy hubs. It provides a decentralized approach based on alternating direction method of multipliers to preserve the ownership when running the optimal scheduling. This could help to keep the privacy and individuality of the microgrids. In [17], a chance-constrained approach is devised for energy management of interconnected microgrids. It proposes a communication based approach for updating the information within the microgrids. The work in [18] tries to find the main technical and economic advantages from the DGs and combined heat and power synchronization in the microgrids. In addition, the role of boilers and fuel cells in supporting part of the thermal loads is discussed. In [19], the authors use the control theory to optimize the amount of reserve power in interconnected microgrids. A good review on the energy management, structure, advantages and features of interconnected microgrids can be found in [20].

One big challenge in front of the progress of the interconnected microgrids is the security of data transactions among the microgrids. In other words, it is always possible that some data get compromised and thus, the entire energy management and sharing process gets affected. This cannot only add to the economic costs; but would also add to the technical and social costs. In [21], a new intrusion detection system based on support vector machine is introduced which is trained by the long-term data recording of the smart meters which can check the health of data received in any time later. The model uses the probabilistic prediction idea for making a feasible domain around the sample data and gives a practical region. In [22], an interval state estimation procedure is developed to create a defense structure against any cyber-attack in the energy internet systems. To this end, deep belief network is deployed for an accurate forecasting of the electrical load demand. This shows the necessity of investigating and taking care of the cyber security of the microgrids, especially in the interconnected mode of operation. In fact, research in the field of secured energy management of microgrids is rare and much more attempts are needed to clarify the different aspects of this problem. Therefore, this article gives a special focus on the optimal scheduling of interconnected microgrids based on the blockchain technology to guarantee the security and optimality of the scheduling solutions. Blockchain, represents an increasing list of data blocks connected to each other through cryptography [23]. In this way, each block has the previous block hash and thus, this links all blocks in a secured way. A novel hybrid method based on stochastic programming of a point estimate method (PEM) is proposed to capture the uncertainty effects due to the renewable energy sources, electrical load demand and energy price. PEM is an efficient and enough accurate method, which tries to make a nonlinear mapping between the input and output of a nonlinear function with the limited number of concentration points [24]. In order to have a practical analysis, a social-economic framework is proposed to not only mitigate the interconnected microgrids operation cost (and thus benefit the customers), but also enhance the social factors such as the average energy not supplied (AENS). Reducing the AENS means a higher social welfare in the region is provided by the interconnected microgrid for the electric consumers [25]. To this end, a reconfiguration strategy is considered as a key solution for changing the topology of microgrids using some remotely control switches [26]. This can not only reduce the power losses in the feeders, but also can reduce the costs by more optimal power sharing among DGs, renewable energy sources and storages [27]. Providing new paths for power supply in a shorter way can also enhance the AENS and thus improve the social factors, appropriately [28]. In order to solve the problem, an effective modified algorithm based on crow search is proposed which helps to find the most optimal operating point for the dispatchable units, the storage unit and microgrids' power sharing scheme. Moreover, a novel modification method is introduced to enhance the algorithm performance by accelerating the search and convergence rate properly. A typical interconnected microgrids with four different residential microgrids is used as the case study to check the model performance.

This paper is organized as follows: section II explains the problem formulation for the proposed social-economic framework. Section IV explains the secured architecture based on blockchain. Section IV explains the proposed stochastic framework based on PEM and corrected crow search (CCS) algorithm. The simulation results are discussed in section V. The main paper outcomes are shown in section VI.

II. SOCIAL-ECONOMIC SCHEDULING OF RECONFIGURABLE INTERCONNECTED MICROGRIDS

In this section, a multi-objective framework is developed for an efficient social and economic operation of the reconfigurable interconnected microgrids. To this end, the objective function is composed of two parts, the AENS as the social objective function, and the total operation cost as the economic objective function. The proposed model optimizes the proposed social-economic indices through some remotely control switches of tie and sectionalizer as well as the optimal output power of the dispatchable units and storages and power exchange among the interconnected microgrids. The economic cost function incorporates the total operation costs of active power losses, cost of DGs and cost of power exchange among the microgrids as below:

$$\begin{aligned} min & \sum_{t\in\Omega^T}\sum_{i\in\Omega^{MG}}\sum_{n\in\Omega_i^N} z_t^M PM_{i,n,t} \\ & + \sum_{t\in\Omega^{Tm}}\sum_{i\in\Omega^{MG}}\sum_{n\in\Omega_i^{NG}} z_{i,n}^G PG_{i,n,t} \\ & + \sum_{t\in\Omega^T}\sum_{mn\in(\Omega^{DF}\cup\Omega^{TF})} z_t^M R_{mn}\left(I_{mn,t}^F\right)^2 \end{aligned} \tag{1}$$

The social AENS as the social objective function is then formulated for the interconnected microgrid as below:

$$Min \sum_{i\in\Omega^{MG}}\left(\sum_{j\in\Omega^{Cus}}^{La_jU_j} / \sum_{j\in\Omega^{Cus}}^{N_j}\right) \tag{2}$$

The problem constraints wherein the above objectives are optimized can then be formulated as below:

A. GENERATION AND DEMAND BALANCE CONSTRAINT

In order guarantee the generation and demand balance in the radial interconnected microgrid, equations (3)-(6) are developed. These constraints are sets of repetitive equations wherein the active and reactive power balances are assured using the KCL and KVL laws. In such a formulation, the auxiliary variable $\Delta V_{mn,t}$ is deployed to simulate the ON/OFF status of the tie switch connecting buses m and n. Therefore, $\Delta V_{mn,t}$ =0 shows that the buses are connected (switch is ON), and any other positive or negative value shows that the switch is off with a specific voltage difference between the two buses.

$$\begin{aligned} & \sum_{km\in(\Omega^{DF}\cup\Omega^{TF})}\left[P_{km,t}^F - R_{km}\left(I_{km,t}^F\right)^2\right] \\ & - \sum_{mn\in(\Omega^{DF}\cup\Omega^{TF})} P_{mn,t}^F + PG_{i,n,t} - P_{i,n,t}^{Ch} \\ & + P_{i,n,t}^{Dch} + PM_{i,n,t} = P_{i,n,t}^D; \forall i\in\Omega^{MG}, \forall n\in\Omega_i^N, \forall t\in\Omega^T \end{aligned} \tag{3}$$

$$\begin{aligned} & \sum_{km\in(\Omega^{DF}\cup\Omega^{TF})}\left[Q_{km,t}^F - X_{km}\left(I_{km,t}^F\right)^2\right] \\ & - \sum_{mn\in(\Omega^{DF}\cup\Omega^{TF})} Q_{mn,t}^F + QG_{i,n,t} \\ & + QM_{i,n,t} = Q_{i,n,t}^D; \forall i\in\Omega^{MG}, \forall n\in\Omega_i^N, \forall t\in\Omega^T \end{aligned} \tag{4}$$

$$\begin{aligned} & \left(V_{i,m,t}\right)^2 - \left(V_{i,n,t}\right)^2 = 2\left(R_{mn}P_{mn,t}^F + X_{mn}Q_{mn,t}^F\right) \\ & - (Z_{mn})^2\left(I_{mn,t}^F\right)^2 + \Delta V_{mn,t} \\ & \forall mn\in\left(\Omega^{DF}\cup\Omega^{TF}\right), \forall t\in\Omega^T \end{aligned} \tag{5}$$

$$\begin{aligned} & \left(V_{i,n,t}\right)^2\left(I_{mn,t}^F\right)^2 = \left(P_{mn,t}^F\right)^2 + \left(Q_{mn,t}^F\right)^2; \\ & \forall mn\in\left(\Omega^{DF}\cup\Omega^{TF}\right), \forall t\in\Omega^T \end{aligned} \tag{6}$$

B. OPERATION CONSTRAINTS

Each bus voltage should be preserved between the limited ranges due to the technical limitations as in (7). The auxiliary voltage $\Delta V_{mn,t}$ can avoid large values by incorporating (8). The amount of power exchange between the interconnected microgrid and the main grid is constrained by (9) and (10). The technical constraints for the dispatchable units are preserved in (11)-(16). In (11) and (12), the minimum and maximum power generations of the DGs, due to the technical limits, are shown. In (13)-(14), the ramp up/down rates for the DGs are considered and the lower up and down time constraints are preserved in (15)-(16). In order to model the battery storage in the interconnected microgrids, constraints (17)-(23) are incorporated in the model. The lower and upper charging/discharging rates for the storage units are represented by (17) and (18), the total storage capacity is constrained by (19) and (20), the timing constraints for the charging/discharging are shown in (21) and (22), and the charging/discharging modes of the energy storage system is represented by (23) as a binary variable.

To model the adjusting load models in the microgrid, constraints (24)-(26) are developed to model either the curtailable/shiftable types. The variable $z_{i,n,t}^{AD}$ shows the status of the adjustable loads to get/not-to-get charged such that the total power demand is supplied in the specific time limit (25). Since the adjustable loads are available in a specific number of hours, constraint (26) is considered to represent this limit.

$$\underline{V} \le V_{i,n,t} \le \overline{V} \quad \forall i\in\Omega^{MG}, \forall n\in\Omega_i^N, \forall t\in\Omega^T \tag{7}$$

$$\begin{aligned} & \left|\Delta V_{mn,t}\right| \le \left(\overline{V} - \underline{V}\right)\left(1 - w_{mn,t}^F\right) \\ & \forall mn\in\left(\Omega^{DF}\cup\Omega^{TF}\right), \quad \forall t\in\Omega^T \end{aligned} \tag{8}$$

$$\begin{aligned} & -\overline{PM_{i,n}}\delta \le PM_{i,n,t}^M \le \overline{PM_{i,n}}\delta \\ & \forall i\in\Omega^{MG}, \quad \forall n\in\Omega_i^N, \forall t\in\Omega^T \end{aligned} \tag{9}$$

$$\begin{aligned} & -\overline{QM_{i,n}}\delta \le QM_{i,n,t} \le \overline{QM_{i,n}}\delta \\ & \forall i\in\Omega^{MG}, \quad \forall n\in\Omega_i^N, \forall t\in\Omega^T \end{aligned} \tag{10}$$

$$\begin{aligned} & \underline{PG_{i,n}}x_{i,n,t}^G \le PG_{i,n,t} \le \overline{PG_{i,n}}x_{i,n,t}^G \\ & \forall i\in\Omega^{MG}, \quad \forall n\in\Omega_i^{NG}, \forall t \end{aligned} \tag{11}$$

$$\begin{aligned} & \underline{QG_{i,n}}x_{i,n,t}^G \le QG_{i,n,t} \le \overline{QG_{i,n}}x_{i,n,t}^G \\ & \forall i\in\Omega^{MG}, \quad \forall n\in\Omega_i^{NG}, \forall t\in\Omega^T \end{aligned} \tag{12}$$

$$PG_{i,n,t} - PG_{i,n,t-1} \le RU^{G}_{i,n} \quad \forall i \in \Omega^{MG}, \quad \forall n \in \Omega^{NG}_{i}, \ \forall t \in \Omega^{T} \tag{13}$$

$$PG_{i,n,t-1} - PG_{i,n,t} \le RD^{G}_{i,n} \quad \forall i \in \Omega^{MG}, \quad \forall n \in \Omega^{NG}_{i}, \ \forall t \in \Omega^{T} \tag{14}$$

$$T^{G-on}_{i,n,t} \ge UT^{G}_{i,n}\left(\alpha^{G}_{i,n,t} - \alpha^{G}_{i,n,t-1}\right) \quad \forall i \in \Omega^{MG}, \quad \forall n \in \Omega^{NG}_{i}, \ \forall t \in \Omega^{T} \tag{15}$$

$$T^{G-off}_{i,n,t} \ge DT^{G}_{i,n}\left(\alpha^{G}_{i,n,t-1} - \alpha^{G}_{i,n,t}\right) \quad \forall i \in \Omega^{MG}, \quad \forall n \in \Omega^{NG}_{i}, \ \forall t \in \Omega^{T} \tag{16}$$

$$\underline{P^{Ch}_{i,n}} y^{Ch}_{i,n,t} \le P^{Ch}_{i,n,t} \le \overline{P^{Ch}_{i,n}} y^{Ch}_{i,n,t} \quad \forall i \in \Omega^{MG}, \quad \forall n \in \Omega^{NS}_{i}, \ \forall t \in \Omega^{T} \tag{17}$$

$$\underline{P^{Dch}_{i,n}} y^{Dch}_{i,n,t} \le P^{Dch}_{i,n,t} \le \overline{P^{Dch}_{i,n}} y^{Dch}_{i,n,t}; \quad \forall i \in \Omega^{MG}, \quad \forall n \in \Omega^{NS}_{i}, \ \forall t \in \Omega^{T} \tag{18}$$

$$C^{S}_{i,n,t} = C^{S}_{i,n,t-1} - P^{Dch}_{i,n,t}\delta/\eta^{Dch}_{i,n} + P^{Ch}_{i,n,t}\delta\eta^{Ch}_{i,n}; \quad \forall i \in \Omega^{MG}, \quad \forall n \in \Omega^{NS}_{i}, \ \forall t \in \Omega^{T} \tag{19}$$

$$\underline{C^{S}_{i,n}} \le C^{S}_{i,n,t} \le \overline{C^{S}_{i,n}} \quad \forall i \in \Omega^{MG}, \quad \forall n \in \Omega^{NS}_{i}, \ \forall t \in \Omega^{T} \tag{20}$$

$$T^{Ch}_{i,n,t} \ge CT^{S}_{i,n}\left(\beta^{Ch}_{i,n,t} - \beta^{Ch}_{i,n,t-1}\right) \quad \forall i \in \Omega^{MG}, \quad \forall n \in \Omega^{NS}_{i}, \ \forall t \in \Omega^{T} \tag{21}$$

$$T^{Dch}_{i,n,t} \ge DT^{S}_{i,n}\left(\beta^{Dch}_{i,n,t} - \beta^{Dch}_{i,n,t-1}\right) \quad \forall i \in \Omega^{MG}, \quad \forall n \in \Omega^{NS}_{i}, \ \forall t \in \Omega^{T} \tag{22}$$

$$y^{Ch}_{i,n,t} + y^{Dch}_{i,n,t} \le 1 \quad \forall i \in \Omega^{MG}, \quad \forall n \in \Omega^{NS}_{i}, \ \forall t \in \Omega^{T} \tag{23}$$

$$\underline{P^{AD}_{i,n}} z^{AD}_{i,n,t} \le P^{D}_{i,n,t} \le \overline{P^{AD}_{i,n}} z^{AD}_{i,n,t}; \quad \forall i \in \Omega^{MG}, \quad \forall n \in \Omega^{BAD}_{i}, \ \forall t \in \Omega^{T} \tag{24}$$

$$\sum_{t \in [\sigma_{i,n}, \omega_{i,n}]} P^{D}_{i,n,t}\delta = E^{AD}_{i,n} \quad \forall i \in \Omega^{MG}, \quad \forall n \in \Omega^{BAD}_{i}, \ \forall t \in \Omega^{T} \tag{25}$$

$$T^{AD-on}_{i,n,t} \ge UT^{AD}_{i,n}\left(z^{AD}_{i,n,t} - z^{AD}_{i,n,t-1}\right) \quad \forall i \in \Omega^{MG}, \forall n \in \Omega^{BAD}_{i}, \forall t \in \Omega^{T} \tag{26}$$

C. RECONFIGURABLE STRUCTURE

Feeder reconfiguration is considered as a precious tool in the interconnected microgrids for changing the power flow and enhancing the objective functions. Nevertheless, it is always preferred to keep the radial structure of the system and get benefits of the radial protection and thus the simple coordination of the protection relays as in (27)-(33). The total number of loops is calculated at any time in the grid by (27). In these equations, the variable $w^{F}_{km,t}$ is used to show the ON/OFF status of the line connecting buses. Moreover, the variable $\theta^{F}_{mn,t}$ is used to avoid any islanded network. Equation (34) is used to avoid high number of switching operation in the microgrid.

$$N_{loop} = N_{branch} - N_{bus} + 1 \tag{27}$$

$$\sum_{km \in (\Omega^{DF} \cup \Omega^{TF})} w^{F}_{km,t} = 1 \quad \forall i \in \Omega^{MG}, \quad \forall n \in \left(\Omega^{BAD}_{i} \cup \Omega^{BCD}_{i}\right), \ \forall t \in \Omega^{T} \tag{28}$$

$$\sum_{km \in (\Omega^{DF} \cup \Omega^{TF})} \theta^{F}_{lm,t} - \sum_{mn \in (\Omega^{DF} \cup \Omega^{TF})} \theta^{F}_{mn,t} + \theta^{M}_{i,m,t} = \theta^{D}_{i,n,t} \quad \forall i \in \Omega^{MG}, \quad \forall t \in \Omega^{T} \tag{29}$$

$$0 \le \theta^{F}_{mn,t} \le \left|\Omega^{N}\right| w^{F}_{mn,t} \ \forall mn \in \Omega^{DF}, \quad \forall t \in \Omega^{T} \tag{30}$$

$$0 \le \theta^{F}_{mn,t} \le \left|\Omega^{N}\right| \ \forall mn \in \Omega^{TF}, \quad \forall t \in \Omega^{T} \tag{31}$$

$$0 \le \theta^{M}_{i,m,t} \le \left|\Omega^{N}\right| \ \forall i \in \Omega^{MG}, \quad \forall n \in \Omega^{N}_{i}, \ \forall t \in \Omega^{T} \tag{32}$$

$$\theta^{D}_{i,n,t} = \begin{cases} 1 \forall i \in \Omega^{MG}, \forall n \in \left(\Omega^{NG}_{i} \cup \Omega^{NS}_{i}\right), \forall t \in \Omega^{T} \\ 0 \forall i \in \Omega^{MG}, \forall n \notin \left(\Omega^{NG}_{i} \cup \Omega^{NS}_{i}\right), \forall t \in \Omega^{T} \end{cases} \tag{33}$$

$$N_{sw} \le \bar{N}_{sw} \forall sw \in \Omega^{Sw} \tag{34}$$

III. SECURED FRAMEWORK BASED ON BLOCKCHAIN

A microgrid consists of a physical layer, with the model explained in the last section, and a communication layer, which works based on a blockchain platform [29]. In such a complex cyber-physical structure, the advanced metering infrastructure (AMI), which works based on wireless sensor networks, is in charge of data gathering, data communication and energy consumption analysis for the optimal operation of the microgrid [30]. In the literature, many platforms exist for Wireless Sensor Networks (WSNs), such as ns-3 and OMNET++. Extensions for these platforms have been created to allow for the simulation of a microgrid cyber layer. In this paper, a blockchain based structure is developed to secure the data transaction among the microgrids in an integrated framework [31]. Blockchain is fundamentally constructed in a distributed topology, in which every microgrid can share its data with the other neighboring connecting microgrids, while no one can control [32]. This makes the data transactions secured against an unauthorized access to the system. Using the advanced cryptography methods, only authorized healthy nodes (microgrids) can access the data exchange among them. Therefore, the critical feature of the blockchain is that it does not need any central unit for the control of the data, a feature that enhances the deep information security. Moreover, a cryptography approach based on hash function is deployed in this method to avoid data access by unauthorized parties in the case of hacking penetration [33]. In a hash system, the input data with a random length is converted into an output bit string with a fixed length. Therefore, the blockchain system main characteristics can be summirized as:

- Data transactions are validated and authorized using an advanced verification approach, which is handled through a decentralized approach.
- Blockchain system does not depend on any specific architecture for connecting microgrids (nodes) and managing them.

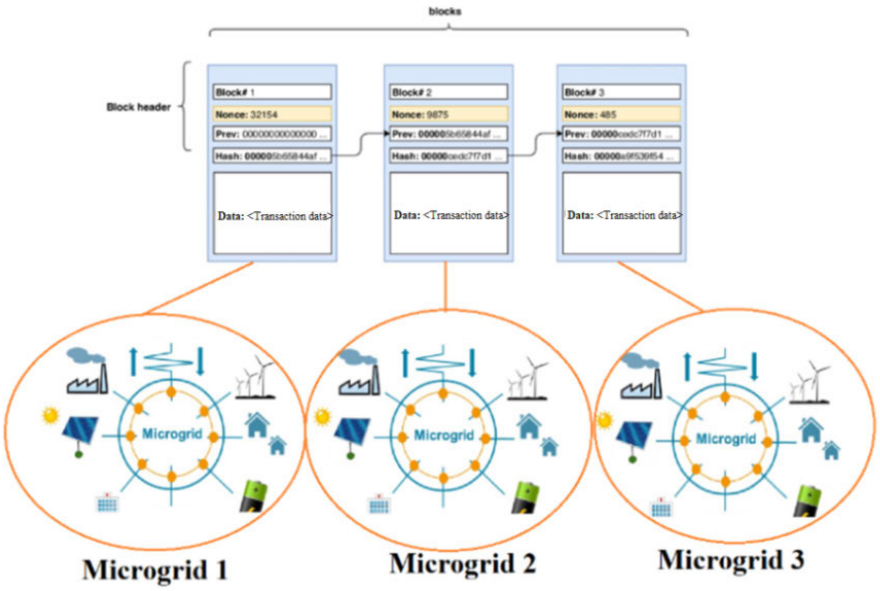

FIGURE 1. Blockchain concept in the interconnected microgrids.

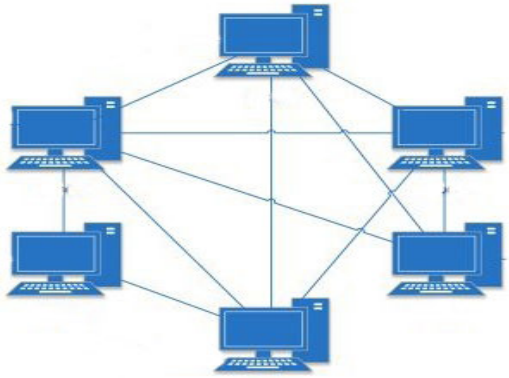

FIGURE 2. The decentralized based peer-to-peer structure.

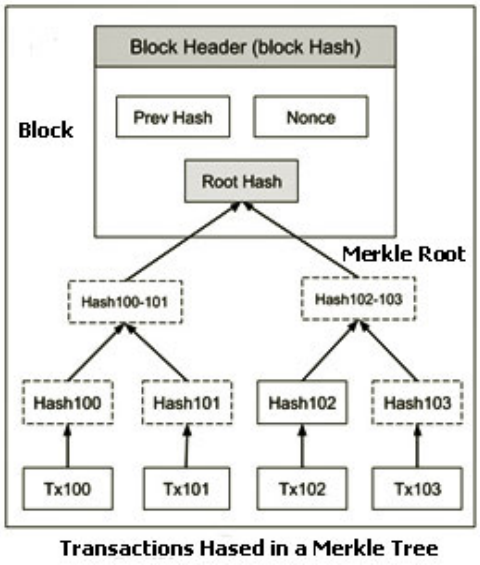

FIGURE 3. Merkle root in the blockchain system.

Fig. 1 shows how the blockchain technology works and is applied to three interconnected microgrids.

The blockchain system can be either private or public, depending on whether the protocol is open access or private to a single entity [34]. Both types are compatible with the interconnected microgrids due to the decentralized (composed of several microgrids) structure. As that is quite needed in the islanding mode of a single microgrid, the blockchain system based on the decentralized framework would let the nodes leave/join the system independently. Figure 2 shows a peer-to-peer structure which is considered for data transaction in the blockchain technology. In the blockchain system, there is a growing record of data, which is defined as blocks that are preserved secure through a nonstop verification [35]. Each block consists of the data transactions among the microgrids, timestamp, the data of the previous block and the Merkle root. Being considered as a critical component in the block header, the Merkle root is the hash of all the hashes of all the transactions. With the help of the Merkle root, one can verify the transaction securely by only downloading the small block header and Merkle tree [36]. Therefore, there is no need to download the entire block data. Fig. 3 shows the Merkle root in the blockchain.

After receiving the data block by a microgrid, it will try to access the embedded information within the block by inserting a specific integer number to the block to create a hash value. It is clear that each microgrid needs to insert the hash values of the previous and current node. The hash function generation is made as a 32-bit value using the standard

hash functions including the SHA-512, SHA-384, SHA-256, SHA-224 and SHA-1. A significant criterion for checking the efficacy of the blockchain system is the time consumption. In order to calculate this value, let us assume the average time used by a node for the preparation of its block data is T_q. Therefore, the overall processing time of blockchain system is calculated as:

$$T_{chain} = T_q \times T_{sig} + (T_{back-off} + T_{trm}) \times 2 + t_{prod} + t_{Mining} \tag{35}$$

where T_{sig} is time elapsed to confirm the signature, $T_{back-off}$ is the back-off time associated with the protocol [37], T_{trm} represents the time used for data transfer from one microgrid to another microgrid, t_{prod} is the time used in order to calculate the data for the block, and t_{Mining} is the time of data block. Considering some delay in the production process, the total blockchain processing time is calculated as below:

$$T_{chain} = T_q \times T_{sig} + (T_{back-off} + T_{trm}) \times 2 + t_{prod} + t_{Mining} \tag{36}$$

IV. STOCHASTIC FRAMEWORK BASED ON PEM AND CORRECTED CROW SEARCH (CCS) ALGORITHM

This section proposes a hybrid evolving stochastic framework based on the point estimate method (PEM) and CCS to solve the optimal scheduling problem in the interconnected microgrids. Considering the discrete nature of the problem, we need to optimize the objective functions during the optimization to find their expected values. Each of these methods is explained in the rest. It should be noted that the nonlinear structure of the proposed problem requires a powerful optimizer to solve it effectively. In this regard, the idea of heuristic algorithms is the most well-known and successful method among the researchers. Among the different optimization methods, CCS has shown some specific features, which makes it a suitable candidate for solving the problem [38]. Powerful local search mechanisms, few setting parameters, fast convergence, simple concept, ease of implementation and compatibility with discrete and continuous optimization methods are the most prominent features of this method [39]. Unfortunately, there is no guarantee for the optimality of the solution in the nonlinear problems. In fact, the main reason for the use of the nonlinear optimization methods such as heuristic algorithms is that these methods can find the most optimal solution among the many unknown optimal solutions in the problem. The other solution is to linearize the problem and then solve it (which of course guarantees the optimality). However, this approach would come at the cost of solution accuracy.

A. STOCHASTIC FRAMEWORK BASED ON 2ρ-PEM

In an interconnected microgrid, the optimal output power of the renewable energy sources, the hourly load demand and forecast error in the market price for the future operation time are the main sources of uncertainty injection. Technically, there are three methods in the stochastic programming for modeling the uncertainty effects. The first method is the Monte Carlo method, which can provide the most accurate uncertainty quantization but with the cost of high computations. The second group is the analytical method which has solved the time consuming nature of the first group but make some assumptions for the uncertain parameters (indeed this would reduce the accuracy). The last group is the approximate methods in which the high accuracy and low time consuming can be both achieved in a single method. The core idea in the approximate methods is using some nonlinear mapping between the input and the output domains using the first few statistical moments in the probability density function (PDF) of the randomness. This article uses the PEM as a well-known and successful approach, in which a problem with ρ uncertain parameter is solved 2ρ times to capture the uncertainty effects [24].

In 2ρ-PEM, each PDF is replaced by two generating points of concentration using the mean and the standard deviation parameters of the uncertainty [40]. Each of these points are then used as an input to the nonlinear problem, let us call it F, to transfer to the arbitrary output objective S:

$$S = F(u) \tag{37}$$

In such a notation, u represents the vector of uncertainty, and S is the output cost function. It is clear that the way that the input u is transferred is quite dependent on the nonlinear problem formulation. Considering f_{ul} as the PDF of the l^{th} uncertainty u_l, 2ρ-PEM will produce two output values as below:

$$S = F(\mu_{u1}, \mu_{u2}, \ldots u_{l,k}, \ldots, \mu_{u\rho}); \quad k = 1, 2 \tag{38}$$

where $u_{l,1}$ and $u_{l,2}$ are the new generating locations for the input uncertain variable u_l, which is computed as below:

$$u_{l,k} = \mu_{u_l} + \vartheta_{l,k} \cdot \sigma_{u_l}; \quad k = 1, 2 \tag{39}$$

In (39), $\vartheta_{l,k}$ shows the standard location for f_{ul}, which is addressed as below:

$$\vartheta_{l,k} = \frac{\psi_{l,3}}{2} + (-1)^{3-k}\sqrt{\rho - (\psi_{l,3}^2/2)^2}, \quad k = 1, 2 \tag{40}$$

$$\psi_{l,3} = \frac{E\left[\left(u_l - \mu_{u_l}\right)^3\right]}{\left(\sigma_{u_l}\right)^3} \tag{41}$$

We have used E as the expectation operator in our notation. After calculating the objective function value for each 2ρ points and thus having 2ρ number of S_i, the characteristics of S can be calculated as below:

$$\sigma = \sqrt{var(S_i)} = \sqrt{E(S_i^2) - [E(S_i)]^2}$$

$$E(S_i^j) = \sum_{l=1}^{\rho}\sum_{k=1}^{2}(\omega_{l,k} \times S_i^j(\mu_{u1}, \mu_{u2}, \ldots, u_{l,k}, \ldots, \mu_{u\rho})) \tag{42}$$

The way that each 2ρ points affect the output value is according to their weighting factors which are calculated as in (43).

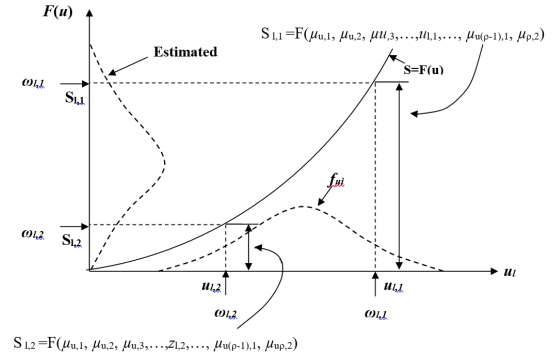

FIGURE 4. The theoretical diagram of 2ρ PEM.

The weighting factor of the right point in the PDF is shown by $\omega_{l,1}$ and the left point is given by $\omega_{l,2}$ as follows:

$$\omega_{l,1} = -\frac{1}{\rho}\frac{\xi_{l,2}}{(\xi_{l,1} - \xi_{l,2})}$$
$$\omega_{l,1} = +\frac{1}{\rho}\frac{\xi_{l,1}}{(\xi_{l,1} - \xi_{l,2})} \quad (43)$$

Fig. 4 shows the illustration of the 2ρ-PEM in the stochastic framework

B. CCS OPTIMIZATION

CCS is a heuristic algorithm which is inspired from the crows' life style in their folks and as they watch other birds for stealing their food in the hidden places. This simple but practical idea has become the core concept for the creation of an effective optimization tool. On the other hand, a bird with the thievery background well knows how to avoid getting the next victim by fooling the crows purchasing her. Moreover, they know well how to hide the food far from the attackers. Therefore, CCS is constructed based on four core ideas [38]:

- Crows have a social life in some flocks
- Any crow can remember food location where it is hidden in
- Crows can find food through a chase and follow up process
- Crows can escape from the chasing bird with some chances CCS starts by generating an initial random population, each representing a possible solution for the problem. After calculating the objective function, the most successful crow is saved as G_{best} and the other members are updated using the above rules [39]:

$$X_i^{Iter+1} = X_i^{Iter} + r_i \times cf_i^{Iter} \times (\alpha_j^{Iter} - X_i^{Iter}) \quad i = 1, \ldots, N \quad (44)$$

where α_j^{Iter} is the food location that is the best situation that a crow could achieve so far. In (44), cf_i^{Iter} is the crow flight length, which helps to adjust the local or global search tendency of the algorithm. Therefore, low values would motivate the CCS to look for the optimal solution in the near domain and large values would motivate the CCS to look for the optimal solution in the far distances. One of the rules in the crow algorithm mentions that a bird which is aware of a chasing crow would try to fool it and does not show its nest. The chance of knowing this is simulated by a probability constant Δ. Therefore, the position of a crow may be updated if she can escape from the chasing birds as below:

$$X_i^{Iter+1} = \begin{cases} X_i^{Iter} + r_i \times fl_i^{Iter} \times (M_j^{Iter} - X_i^{Iter}); & r_j \geq \Delta_j^{Iter} \\ X^{rand}; & r_j \prec \Delta_j^{Iter} \end{cases} \quad (45)$$

The Δ is a significant parameter, which can maintain the randomness of the algorithm. A large value of Δ simulates searches that are more random or the global search.

Although the CCS is an appropriate algorithm for solving the nonlinear problems, it suffers from some issues. The first issue is about the *cf* value, which can affect directly the local and global search ability of the algorithm. Technically, it is more preferred to have global search at the beginning of the optimization to better analyze the search domain and later make local search around the available optimal solutions. Therefore, an experimental formulation is developed for *cf* to update its value and meet the above preferences.

$$cf_i^{Iter+1} = cf_i^0 \times e^{-Iter} \quad (46)$$

where cf_i^0 is the initial *cf* value.

The second issue in the CCS is the constant parameter Δ. This parameter can also affect the algorithm performance and is assumed constant all the time. To overcome this issue, a dynamic formulation has been devised to adjust its optimal value dynamically:

$$\Delta_i^{Iter+1} = \Delta_i^0 \left(1 - \frac{1}{e^{\partial \times Iter}}\right) \quad (47)$$

where ∂ is a constant value, and Δ_i^0 is the initial value of Δ.

In order to increase the diversity of the crow population and thus enhance the chance of a uniform search, the crossover and mutation operators are borrowed from genetic algorithm and deployed as below. Three different test solutions are produced as below:

$$x_{Test\,1,j} = \begin{cases} x_{i,j}; & \delta_2 \leq \delta_3 \\ x_{Gbest,j}; & \text{else} \end{cases} \quad (48)$$
$$X_{i,j} = [x_{i,1}, x_{i,2}, \ldots, x_{i,d}]_{1\times d}$$
$$x_{Test2,j} = \begin{cases} x_{i,j}; & \delta_3 \leq \delta_4 \\ x_j; & \text{else} \end{cases} \quad (49)$$
$$X_{Test,3} = G_{best} + \delta_4 \times (G_{best} - X_i) \quad (50)$$

The most fitting solution would replace the X_i crow in the population.

V. SIMULATION RESULTS

In this section, an interconnected microgrid test system is simulated and analyzed to check the proposed model quality and performance. The test system has seventy-three switches,

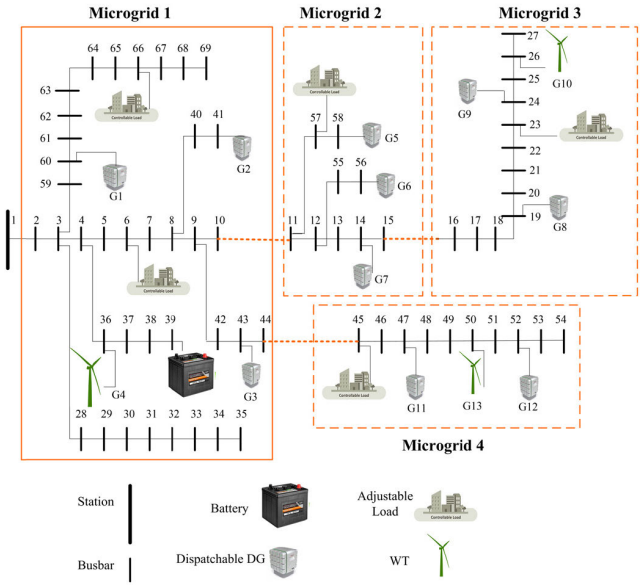

FIGURE 5. One-line diagram of the test networked MG system.

TABLE 1. Characteristics of DGs.

	Unit	Type	Cost ($/kWh)	Min-Max Power (kW)	Up/Down Time (h)	Ramp Up/Down (kW/h)
MG 1	DG1	D	0.156	800-2500	3	1400
	DG2	D	0.169	500-3200	3	1400
	DG3	D	0.187	800-2200	2	1000
	DG4	ND	-	0-1400	-	-
MG 2	DG5	D	0.153	800-1800	3	1300
	DG6	D	0.145	800-1800	3	1300
	DG7	D	0.186	800-2200	3	1300
MG 3	DG8	D	0.215	500-2200	3	1000
	DG9	D	0.188	700-3000	2	1400
	DG10	ND	-	0-2100	-	-
MG 4	DG11	D	0.173	700-3000	3	1400
	DG12	D	0.197	500-2200	3	1200
	DG13	ND	-	0-1600	-	-

among which sixty-eight are sectionalizing switches and five are tie switches. Fig. 5 shows the diagram of the test system [41]. There are four microgrids in the test system, which are connected to each other through the red dotted lines. The data characteristics of the interconnected microgrid are provided in Table 1. Here, the symbols D and ND refer to the dispatchable and non-dispatchable units, respectively. The only non-dispatchables unit is wind turbine which exists in the microgrid 1, 3 and 4. Table 2 shows the features of the storage unit located at bus 39. The battery storage is assumed to keep either charging/discharging for five successive hours. The shiftable and curtailable loads are shown in Table 3. It is clear that these loads can help much in mitigating the negative effect of the peak loads.

Figures 6 to 8 show the hourly forecast values of the electrical load factor, wind turbine output power and market price, respectively. In order to have a fair comparison, three different scenarios are simulated here:

TABLE 2. Energy storage characteristics.

Storage	Capacity (kWh)	Min/Max Charging/Discharging Power (kW)	Min Charging/Discharging Time (h)
DES	2000	50-200	5

TABLE 3. Adjustable loads characteristics.

Load	Type	Min-Max Capacity (kW)	Required Energy (kWh)	Initial Start/End Time (h)	Min Up Time
L1(MG1)	SHIFTABLE	0-150	480	9-13	1
L2(MG2)	SHIFTABLE	0-110	310	14-18	1
L3(MG3)	SHIFTABLE	20-80	220	13-17	1
L4(MG4)	CURTAILABLE	10-60	340	1-24	12
L5(MG5)	CURTAILABLE	30-80	400	13-24	12

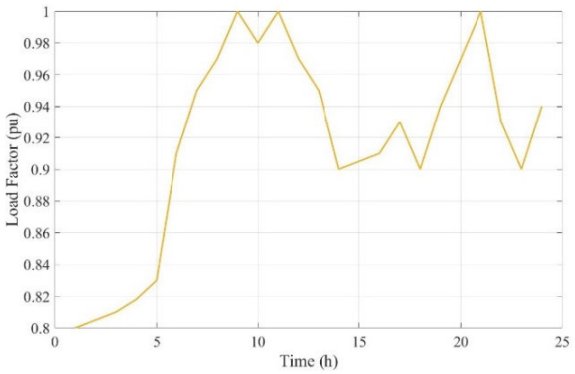

FIGURE 6. Hourly forecast value of the electrical load factor.

- Scenario I: Considering only the economic objective and ignoring the social preferences (AENS)
- Scenario II: Considering only the social objective and ignoring the economic preferences (Cost)
- Scenario III: Considering the social-economic objectives simultaneously.

The results of simulations are discussed in the rest.

***Scenario I*:** This scenario only optimizes the cost function and thus has a special focus on the economic preferences regardless of the social concerns. Table 4 shows the optimal scheduling of the adjustable loads for 24 hours. As it can be seen from the results, the scheduling tendency is toward more distributed demand supply, which can mitigate the peak-load hours and avoid feeder congestion. The optimal scheduling of the units in the microgrids is shown in Table 5. According to these results, the interconnected microgrid is more interested in making use of the economic units with lower marginal costs to minimize the operation costs. In contrast, the interconnected microgrid tries to turn off units with high marginal cost and mitigate the total operating cost at the light-load hours. The power units 1 and 6 with the lowest marginal cost have been fully engaged in the power supply at all hours of the day. On the next step, units 9 and 11 have committed the most to the optimal scheduling program from the cost perspective. Unit number 12 is completely shut down due to the high cost values. The energy storage is charging at the light load hours

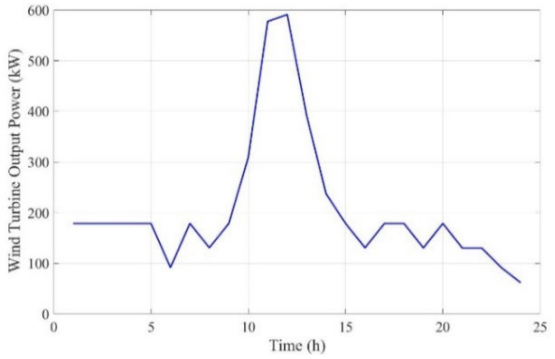

FIGURE 7. Hourly forecast value of the wind turbine output power.

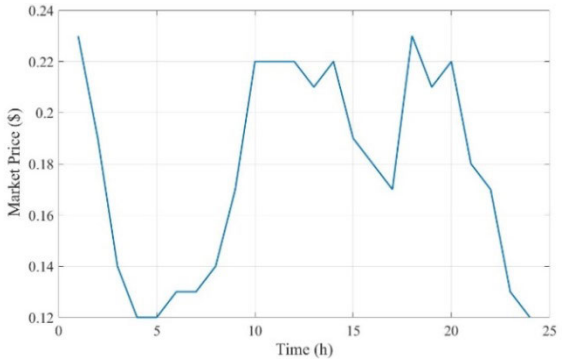

FIGURE 8. Hourly forecast value of the market price.

TABLE 4. Optimal Scheduling of Adjustable Loads in Scenario I and II.

D1	0	0	0	0	0	0	0	0	1	1	1	1	1	0	0	0	0	0	0	0	0	0	0	0
D2	0	0	0	0	0	0	0	0	0	0	0	0	0	1	1	1	1	1	0	0	0	0	0	0
D3	0	0	0	0	0	0	0	0	0	0	0	0	1	1	1	1	1	0	0	0	0	0	0	0
D4	1	1	1	1	1	1	1	1	1	1	1	1	1	1	1	1	1	1	1	1	1	1	1	1
D5	0	0	0	0	0	0	0	0	0	0	0	0	1	1	1	1	1	1	1	1	1	1	1	1

TABLE 5. Optimal Scheduling of Dispatchable Units in the Interconnected Microgrid and scenario I.

	Hours (1-24)																							
DG1	1	1	1	1	1	1	1	1	1	1	1	1	1	1	1	1	1	1	1	1	1	1	1	1
DG2	0	1	1	1	0	0	0	0	1	1	1	1	0	1	1	1	0	0	0	1	1	1	1	0
DG3	0	0	0	0	0	0	0	0	0	0	0	0	0	0	0	0	0	0	0	0	0	0	0	0
DG5	0	0	0	0	0	0	0	1	1	1	1	1	0	0	0	0	0	0	0	0	0	0	0	0
DG6	1	1	1	1	1	1	1	1	1	1	1	1	1	1	1	1	1	1	1	1	1	1	1	0
DG7	0	0	0	0	0	0	0	0	0	0	0	0	0	0	0	0	0	0	0	0	0	0	0	0
DG8	0	0	0	0	0	0	0	0	0	0	0	0	0	0	0	0	0	0	0	0	0	0	0	0
DG9	0	0	0	1	1	1	1	1	1	1	1	1	1	1	1	1	1	1	1	1	1	1	1	1
DG11	0	0	0	1	1	1	1	1	1	1	1	1	1	1	1	1	1	1	1	1	1	1	1	1
DG12	0	0	0	0	0	0	0	0	0	0	0	0	0	0	0	0	0	0	0	0	0	0	0	0
DES	-1	-1	-1	-1	-1	-1	-1	1	1	1	1	1	-1	-1	-1	-1	-1	-1	1	1	1	1	1	1

to discharge at the peak hours and reduce the high cost by more internal power supply. The total microgrid operation cost is $21,714 and AENS is 1.452 kWh/customer.yr.

***Scenario II*:** This scenario optimizes the social target based on the AENS to enhance the power quality services to the network consumers. Applying the social preferences reduces the attention to the operation cost and enhances the amount of energy which is expected to be supplied to the end users. Table 6 shows the status of the units in the second scenario. According to these results, the power dispatch is more shifted to units with closer distance to the end users and thus it is seen that expensive unis like 8 and 12 are attending the microgrid power generation at some hours. Therefore, one can see brighter role for microgrids 3 and 4 in this scenario rather the previous scenario. On the other hand, units 6 and 9 with lower marginal cost are less deployed for power generation compared to the previous scenario. This mainly roots in the nature of the social objective function which depends on the failure rate of the components rather than the cost of units. The dispatchable units' scheduling is the same as unit 1 as shown in Table 4. The optimal values of the AENS and cost functions are 1.324 kWh/customer.yr and $22,835, respectively.

TABLE 6. Optimal Scheduling of Dispatchable Units in the Interconnected Microgrid in scenario II.

	Hours (1-24)																							
DG1	1	1	1	1	1	1	1	1	1	1	1	1	1	1	1	1	1	1	1	1	1	1	1	1
DG2	0	1	1	1	0	0	1	1	1	1	1	0	1	1	1	0	0	0	1	1	1	1	0	
DG3	0	0	0	0	1	1	1	1	1	0	0	0	0	0	0	0	0	0	0	0	0	0	0	0
DG5	0	0	0	0	0	0	0	1	1	1	1	1	0	0	0	0	0	0	0	0	0	0	0	0
DG6	1	1	1	1	1	1	1	0	1	0	0	1	0	0	1	1	1	1	1	1	1	1	0	0
DG7	0	0	0	0	0	0	0	0	0	0	0	1	0	1	1	1	0	1	1	0	0	0	0	0
DG8	0	0	0	0	0	0	0	0	0	0	0	0	0	0	0	0	0	0	0	0	0	0	0	0
DG9	0	0	0	1	1	1	1	0	0	0	0	1	1	1	1	1	1	1	1	1	1	1	1	1
DG11	0	0	0	1	1	1	1	1	1	1	1	1	1	1	1	1	1	1	1	1	1	1	1	1
DG12	0	0	0	0	0	0	0	1	1	1	0	1	1	1	1	0	0	0	0	0	0	0	0	0
DES	-1	-1	-1	-1	-1	-1	-1	1	1	1	1	1	-1	-1	-1	-1	-1	-1	-1	1	1	1	1	1

Scenario III: In this scenario, the interconnected microgrid is operated in a multi-objective framework using the fuzzy min-max approach to progress the social-economic objectives. The conflicting behavior of the social and economic targets could be seen from the previous scenarios. By the use of this min-max framework, the optimization framework tries to optimize both objectives in a way that both are benefited during the power scheduling plan. Table 7 shows the status of the adjustable loads in this scenario. It can be seen that adjustable loads D1 and D3 have some changes in their scheduling but other loads have remained unchanged. This is mainly due to the social-economic framework, which has affected the power generation pattern of some DG units in the system. Table 8 shows the optimal scheduling of the DGs in a multi-objective social-economic framework. According to these results, it can be seen that all units have committed in the scheduling program with a notable change in On/OFF hours for DGs and charging/discharging hours for the DES. The total operation cost and AENS are $21,935 and 1.352 kWh/customer.yr, respectively, which proves a suitable trade-off between the previous scenarios.

The interconnected microgrid topology after the reconfiguration in scenario III is shown in Table 9. The role of reconfiguration has been considered in all cases, but the results are only shown in this scenario to avoid repetition. In this table, only active switches, switches which have

TABLE 7. Optimal Scheduling of Adjustable Loads in Scenario III.

D1	0	0	0	0	0	0	0	0	1	1	1	0	1	0	0	0	0	0	0	0	0	0	0	0
D2	0	0	0	0	0	0	0	0	0	0	0	0	0	1	1	1	1	1	0	0	0	0	0	0
D3	0	0	0	0	0	0	0	0	0	0	0	0	1	1	0	1	0	0	0	0	0	0	0	0
D4	1	1	1	1	1	1	1	1	1	1	1	1	1	1	1	1	1	1	1	1	1	1	1	1
D5	0	0	0	0	0	0	0	0	0	0	0	0	1	1	1	1	1	1	1	1	1	1	1	1

TABLE 8. Optimal Scheduling of Dispatchable Units in the Interconnected Microgrid and scenario III.

	Hours (1-24)																							
DG1	1	1	1	1	1	1	1	1	1	1	1	1	1	1	1	1	1	1	1	1	1	1	1	1
DG2	0	0	1	0	0	0	0	0	1	1	1	1	0	1	1	1	0	0	0	1	1	1	1	1
DG3	0	0	0	0	0	0	0	0	0	0	0	0	0	0	0	0	0	0	0	0	0	0	0	0
DG5	0	0	0	0	0	0	1	1	1	1	1	1	1	0	0	0	0	0	0	0	0	0	0	0
DG6	0	0	0	1	1	1	1	1	1	1	1	1	1	1	1	1	1	1	1	1	1	1	0	0
DG7	0	0	0	0	0	0	0	0	0	0	0	0	0	0	0	0	0	0	0	0	0	0	0	0
DG8	0	0	0	0	0	0	0	0	0	0	0	0	0	0	0	0	0	0	0	0	0	0	0	0
DG9	0	0	0	0	1	1	1	1	1	1	1	1	1	1	1	1	1	1	0	1	1	1	1	0
DG11	0	0	0	0	1	1	1	1	1	1	1	1	1	1	1	0	1	1	1	1	1	1	1	1
DG12	0	0	0	0	0	0	0	0	0	0	0	0	0	0	0	0	0	0	0	0	0	0	0	0
DES	-1	-1	-1	-1	-1	-1	1	1	1	1	1	-1	-1	-1	-1	-1	-1	1	1	1	1	1	1	1

TABLE 9. Switching Status During the Reconfiguration in Scenario III.

	Hours (1-24)																							
Sectionalizing Switches	2	0	0	0	0	0	0	0	0	0	0	0	0	0	0	0	0	0	0	0	1	0	0	0
	6	0	0	0	1	0	0	0	0	0	0	0	0	0	0	0	0	0	0	0	0	0	1	0
	9	0	1	0	0	0	0	0	0	0	0	0	0	0	0	0	0	0	0	0	0	0	0	0
	12	0	0	0	0	0	0	0	0	0	0	1	0	0	0	1	0	0	0	0	0	0	0	0
	13	0	0	0	0	0	0	0	0	0	1	0	0	0	0	0	0	0	0	0	0	0	0	0
	14	1	0	0	0	0	0	0	1	0	0	0	0	0	0	0	0	0	1	0	0	0	0	0
	16	0	0	0	0	0	0	0	0	1	0	0	0	0	0	1	0	0	0	0	0	0	0	0
	18	0	0	1	0	0	1	0	0	0	0	0	0	0	0	0	0	0	1	0	1	0	0	0
	20	0	1	0	0	0	0	0	0	0	0	0	1	0	0	0	0	1	0	0	0	0	0	0
	23	0	0	0	0	0	0	0	0	0	0	1	0	0	0	1	0	0	0	0	0	0	0	0
	26	0	0	0	0	1	0	0	0	0	0	0	0	0	0	0	0	0	0	0	0	0	0	0
	29	0	0	0	0	0	0	1	0	0	0	0	0	0	0	0	1	0	1	0	0	0	0	0
	30	0	0	0	0	0	0	0	0	0	0	0	0	1	0	0	0	0	0	0	0	0	0	1
	33	0	0	0	0	0	0	0	0	0	0	0	0	0	1	0	0	1	0	0	0	0	0	0
	36	0	0	0	0	0	1	0	0	0	0	0	0	0	0	0	0	0	0	0	0	0	0	0
	38	0	0	1	0	0	0	0	0	0	0	0	0	0	0	0	0	0	0	0	0	0	1	0
	47	0	0	0	0	1	0	0	0	0	0	0	0	0	0	0	0	0	0	0	0	0	0	0
	49	0	0	0	0	0	0	1	0	0	0	0	1	0	0	0	1	0	0	0	0	0	0	0
	52	0	0	0	0	0	0	0	0	1	0	0	0	0	0	0	0	0	0	0	0	0	0	0
	57	0	0	0	0	0	0	0	0	0	0	0	1	0	0	0	0	0	0	0	0	0	0	0
Tie Switches	69	1	1	1	0	1	0	1	1	1	0	0	1	1	1	0	1	1	1	1	0	1	0	1
	70	1	1	0	1	1	0	0	1	1	1	1	1	0	0	1	0	0	0	1	1	1	0	1
	71	1	1	1	1	1	1	1	0	0	1	1	0	1	1	1	0	1	1	0	1	1	1	1
	72	1	0	0	1	0	1	1	1	1	0	1	0	1	0	1	0	0	1	1	1	0	1	1
	73	0	0	1	1	0	1	0	1	0	1	1	0	1	1	1	1	1	1	0	1	1	1	0

experienced an operation, are shown. Therefore, other switches that are not shown here have remained unchanged. The values 0 and 1 are used here to show the closed and open status, respectively. As it can be seen from this table, all tie switches are operating actively to alter the microgrid topology and enhance the optimal values of the objective functions. Through the optimal switching, the total operation cost has reduced from \$22,716 to \$21,935 (3.56% reduction) and the AENS has reduced from 1.4115 to 1.352 kWh/customer.yr (4.40% reduction). Such notable values advocate the high effect of the reconfiguration on the social-economic framework.

In order to check the stochastic framework performance for handling the uncertainty effects, Figs. 9 and 10 show the comparative plot of the cost and AENS for the last scenario. According to these results, the optimal values of the cost

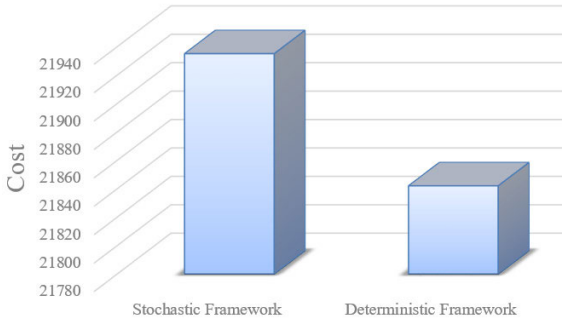

FIGURE 9. Uncertainty effect on the total operation cost in scenario III using the proposed stochastic framework.

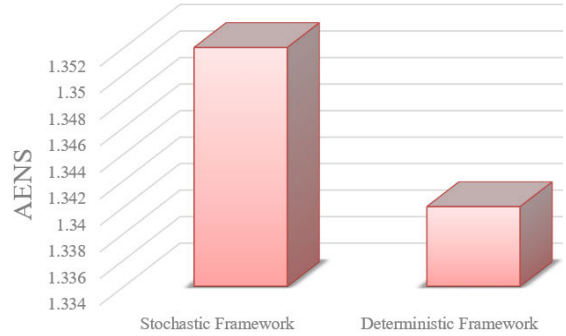

FIGURE 10. Uncertainty effect on the AENS in scenario III using the proposed stochastic framework.

and AENS have increased when incorporating the uncertainty effects. This shows the necessity of the stochastic programming and that ignoring the uncertainty can result in unrealistic scheduling and operation.

In order to better test the algorithm performance, Table 10 is considered. In this table, the total operation cost in scenario III is solved for 20 trails using the proposed stochastic framework and the results of the best solution, the worst solution, standard deviation and CPU time are provided. To have better comparison, the results of the genetic algorithm (GA) [42],[43] particle swarm optimization (PSO) [44],[45] and original CCS algorithm are provided in the table. According to these results, the proposed modified CCS could get to a more optimal solution which is not attained by any other algorithms. This shows that GA, PSO and original CCS have trapped in the local optima. Moreover, the low standard deviation value and CPU time show the high robustness of the algorithm with much lower computational burden.

Finally, Table 11 shows the total processing time of the secured blockchain system for data transaction in all scenarios. Moreover, the computational burden on the central control unit for optimal scheduling is provided comparatively. According to these results, the proposed blockchain based secured framework requires very low computational processing time, which is quite compatible with the hourly operation and scheduling problem. The higher data transferring time in the second scenario compared to the first scenario is due to the higher amount of data to be exchanged

TABLE 10. Comparing the Performance of the proposed algorithm with original CCS, GA and PSO in the stochastic framework for scenario III.

Method	Best Solution	Worst Solution	Standard Deviation	CPU Time
GA	22215	22413	195.25	13.163
PSO	22005	22163	143.62	11.739
CCS	22056	22175	98.60	10.127
Modified CCS	21935	21996	43.62	8.074

TABLE 11. Total processing time of blockchain in the interconnected microgrid.

Method	T_{chain} (s)	CPU Time (s)
Scenario I	1.24	11.70
Scenario II	1.34	10.64
Scenario III	1.39	13.35

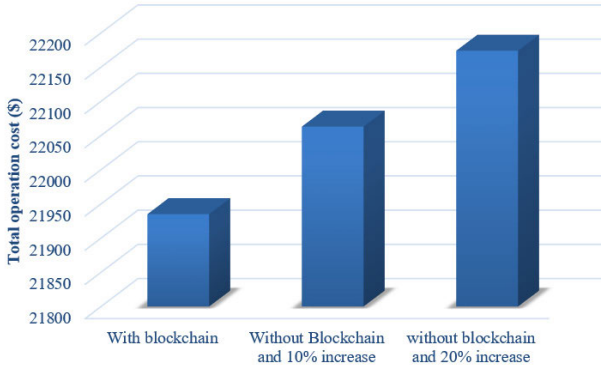

FIGURE 11. Effect of blockchain on the system operation when cyber-attack on the system.

when computing the social target, i.e. AENS (failure rate and repair rate of all components). The amount of data required to be transferred for the social-economic operation of the interconnected microgrid is the most, which is reflected on T_{chain}.

The negligence of blockchain can affect the entire security of the system ranging from the generation to the consumption components. Therefore, the way that energy management system is affected differs depending on the cyber-attack type and model. Here, we consider one type of cyber-attack, namely false data injection attack, which can compromise the system data in the lack of blockchain technology. The cyber hacking point is the system load factor at hours 15 and 16 with 20% increase by the hacker in the small steps of 10%. Therefore, the microgrid would tend to generate more power at these hours while there is not any need to make such an increase in the power generation. The total cost of the microgrid for these hours is shown in Fig. 11. It is clear that the system has faced an unexpected increase in the operation cost when there is no need to the extra power generation. This is due to the fake increase in the load power factor at two successive hours, which has resulted in extra power generation in the relevant hours as well as increasing the cost.

VI. CONCLUSION

Secured optimal scheduling and operation of the interconnected microgrids is a significant and challenging problem for the operators of the power system. This article proposed a novel secured blockchain based stochastic framework for social-economic operation of the interconnected microgrids. To this end, a comprehensive model incorporating the network topology, dispatchable and non-dispatchable units (wind turbine), DESs, tie and sectionalizing switches and adjustable loads (shiftable and curtailable) is proposed. Three different scenarios are defined and analyzed to assess the different aspects of the model. The results show that a social-economic framework can provide an appropriate trade-off between these two conflicting targets. It was seen that the proposed stochastic method could optimize the AENS and the total operation cost effectively. From the switching point of view, the remotely controlled switches of tie and sectionalizing could enhance the AENS and cost by 3.56% and 4.40% reduction, respectively. The proposed blockchain based framework requires very limited computational processing time, which is quite suitable for the hourly scheduling program of the interconnected microgrids. From the uncertainty point of view, ignoring the forecast error in the random parameters of the problem can result in unrealistic values, far from the practical values of the cost and AENS objectives. The proposed problem formulation in this paper is constructed based on a centralized structure and thus is not compatible with the distributed structures. All formulations and objective functions are only applicable for the traditional centralized systems. The authors would address this issue in the future works.

ACKNOWLEDGMENT

The authors gratefully acknowledge the approval and the support of this research study by Taif University Researchers Supporting Project number (TURSP-2020/34), Taif University, Taif, Saudi Arabia.

REFERENCES

[1] T. Lan, K. Jermsittiparsert, S. T. Alrashood, M. Rezaei, L. Al-Ghussain, and M. A. Mohamed, "An advanced machine learning based energy management of renewable microgrids considering hybrid electric vehicles' charging demand," *Energies*, vol. 14, no. 3, p. 569, Jan. 2021.

[2] S. Esmaeili, A. Anvari-Moghaddam, S. Jadid, and J. M. Guerrero, "Optimal simultaneous day-ahead scheduling and hourly reconfiguration of distribution systems considering responsive loads," *Int. J. Electr. Power Energy Syst.*, vol. 104, pp. 537–548, Jan. 2019.

[3] M. A. Mohamed, T. Jin, and W. Su, "Multi-agent energy management of smart islands using primal-dual method of multipliers," *Energy*, vol. 208, Oct. 2020, Art. no. 118306.

[4] M. Hemmati, B. Mohammadi-Ivatloo, M. Abapour, and A. Anvari-Moghaddam, "Optimal chance-constrained scheduling of reconfigurable microgrids considering islanding operation constraints," *IEEE Syst. J.*, vol. 14, no. 4, pp. 5340–5349, Dec. 2020.

[5] N. Bazmohammadi, A. Anvari-Moghaddam, A. Tahsiri, A. Madary, J. C. Vasquez, and J. M. Guerrero, "Stochastic predictive energy management of multi-microgrid systems," *Appl. Sci.*, vol. 10, no. 14, p. 4833, Jul. 2020.

[6] S. Esmaeili, A. Anvari-Moghaddam, and S. Jadid, "Optimal operational scheduling of reconfigurable multi-microgrids considering energy storage systems," *Energies*, vol. 12, no. 9, p. 1766, May 2019.

[7] P. Wang, D. Wang, C. Zhu, Y. Yang, H. M. Abdullah, and M. A. Mohamed, "Stochastic management of hybrid AC/DC microgrids considering electric vehicles charging demands," *Energy Rep.*, vol. 6, pp. 1338–1352, Nov. 2020.

[8] M. Hemmati, B. Mohammadi-Ivatloo, M. Abapour, and A. Anvari-Moghaddam, "Day-ahead profit-based reconfigurable microgrid scheduling considering uncertain renewable generation and load demand in the presence of energy storage," *J. Energy Storage*, vol. 28, Apr. 2020, Art. no. 101161.

[9] M. A. Mohamed, H. Chabok, E. M. Awwad, A. M. El-Sherbeeny, M. A. Elmeligy, and Z. M. Ali, "Stochastic and distributed scheduling of shipboard power systems using MθFOA-ADMM," *Energy*, vol. 206, Sep. 2020, Art. no. 118041.

[10] M. A. Mohamed, T. Jin, and W. Su, "An effective stochastic framework for smart coordinated operation of wind park and energy storage unit," *Appl. Energy*, vol. 272, Aug. 2020, Art. no. 115228.

[11] M. J. Hossain, M. A. Mahmud, F. Milano, S. Bacha, and A. Hably, "Design of robust distributed control for interconnected microgrids," *IEEE Trans. Smart Grid*, vol. 7, no. 6, pp. 2724–2735, Nov. 2016.

[12] N. Bazmohammadi, A. Tahsiri, A. Anvari-Moghaddam, and J. M. Guerrero, "Stochastic predictive control of multi-microgrid systems," *IEEE Trans. Ind. Appl.*, vol. 55, no. 5, pp. 5311–5319, Sep. 2019.

[13] M. Daneshvar, B. Mohammadi-Ivatloo, S. Asadi, A. Anvari-Moghaddam, M. Rasouli, M. Abapour, and G. B. Gharehpetian, "Chance-constrained models for transactive energy management of interconnected microgrid clusters," *J. Cleaner Prod.*, vol. 271, Oct. 2020, Art. no. 122177.

[14] X. Kong, D. Liu, C. Wang, F. Sun, and S. Li, "Optimal operation strategy for interconnected microgrids in market environment considering uncertainty," *Appl. Energy*, vol. 275, Oct. 2020, Art. no. 115336.

[15] M. Daneshvar, B. Mohammadi-Ivatloo, K. Zare, and S. Asadi, "Transactive energy management for optimal scheduling of interconnected microgrids with hydrogen energy storage," *Int. J. Hydrogen Energy*, Oct. 2020.

[16] N. Nikmehr, "Distributed robust operational optimization of networked microgrids embedded interconnected energy hubs," *Energy*, vol. 199, May 2020, Art. no. 117440.

[17] N. Bazmohammadi, A. Tahsiri, A. Anvari-Moghaddam, and J. M. Guerrero, "A hierarchical energy management strategy for interconnected microgrids considering uncertainty," *Int. J. Electr. Power Energy Syst.*, vol. 109, pp. 597–608, Jul. 2019.

[18] A. Anestis and V. Georgios, "Economic benefits of smart microgrids with penetration of DER and mCHP units for non-interconnected islands," *Renew. Energy*, vol. 142, pp. 478–486, Nov. 2019.

[19] D. H. Tungadio and R. C. Bansal, "Active power reserve estimation of two interconnected microgrids," *Energy Procedia*, vol. 105, pp. 3909–3914, May 2017.

[20] H. Zou, S. Mao, Y. Wang, F. Zhang, X. Chen, and L. Cheng, "A survey of energy management in interconnected multi-microgrids," *IEEE Access*, vol. 7, pp. 72158–72169, 2019.

[21] M. A. Mohamed, H. M. Abdullah, M. A. El-Meligy, M. Sharaf, A. T. Soliman, and A. Hajjiah, "A novel fuzzy cloud stochastic framework for energy management of renewable microgrids based on maximum deployment of electric vehicles," *Int. J. Electr. Power Energy Syst.*, vol. 129, Jul. 2021, Art. no. 106845.

[22] H. Wang, J. Ruan, Z. Ma, B. Zhou, X. Fu, and G. Cao, "Deep learning aided interval state prediction for improving cyber security in energy Internet," *Energy*, vol. 174, pp. 1292–1304, May 2019.

[23] C. Walsh, P. O'Reilly, R. Gleasure, J. McAvoy, and K. O'Leary, "Understanding manager resistance to blockchain systems," *Eur. Manage. J.*, Oct. 2020.

[24] R. Sedaghati and A. Kavousi-Fard, "A hybrid fuzzy-PEM stochastic framework to solve the optimal operation management of distribution feeder reconfiguration considering wind turbines," *J. Intell. Fuzzy Syst.*, vol. 26, no. 4, pp. 1711–1721, 2014.

[25] T. Kovaltchouk, A. Blavette, J. Aubry, H. B. Ahmed, and B. Multon, "Comparison between centralized and decentralized storage energy management for direct wave energy converter farm," *IEEE Trans. Energy Convers.*, vol. 31, no. 3, pp. 1051–1058, Sep. 2016.

[26] A. Kavousi-Fard, M. Wang, and W. Su, "Stochastic resilient post-hurricane power system recovery based on mobile emergency resources and reconfigurable networked microgrids," *IEEE Access*, vol. 6, pp. 72311–72326, 2018.

[27] X. Gong, F. Dong, M. A. Mohamed, O. M. Abdalla, and Z. M. Ali, "A secured energy management architecture for smart hybrid microgrids considering PEM-fuel cell and electric vehicles," *IEEE Access*, vol. 8, pp. 47807–47823, 2020.

[28] S. Ouadfel and M. A. Elaziz, "Enhanced crow search algorithm for feature selection," *Expert Syst. Appl.*, vol. 159, Nov. 2020, Art. no. 113572.

[29] K. Gai, J. Guo, L. Zhu, and S. Yu, "Blockchain meets cloud computing: A survey," *IEEE Commun. Surveys Tuts.*, vol. 22, no. 3, pp. 2009–2030, 3rd Quart., 2020.

[30] X. Gong, F. Dong, M. A. Mohamed, E. M. Awwad, H. M. Abdullah, and Z. M. Ali, "Towards distributed based energy transaction in a clean smart island," *J. Cleaner Prod.*, vol. 273, Nov. 2020, Art. no. 122768.

[31] Q. Duan, N. V. Quynh, H. M. Abdullah, A. Almalaq, T. D. Do, S. M. Abdelkader, and M. A. Mohamed, "Optimal scheduling and management of a smart city within the safe framework," *IEEE Access*, vol. 8, pp. 161847–161861, 2020.

[32] M. Belotti, N. Bozic, G. Pujolle, and S. Secci, "A vademecum on blockchain technologies: When, which, and how," *IEEE Commun. Surveys Tuts.*, vol. 21, no. 4, pp. 3796–3838, Jul. 2019.

[33] A. V. Tutueva, A. I. Karimov, L. Moysis, C. Volos, and D. N. Butusov, "Construction of one-way hash functions with increased key space using adaptive chaotic maps," *Chaos, Solitons Fractals*, vol. 141, Dec. 2020, Art. no. 110344.

[34] Z. Zheng, S. Xie, H. Dai, X. Chen, and H. Wang, "An overview of blockchain technology: Architecture, consensus, and future trends," in *Proc. IEEE Int. Congr. Big Data (BigData Congress)*, Jun. 2017, pp. 557–564.

[35] M. Andoni, V. Robu, D. Flynn, S. Abram, D. Geach, D. Jenkins, P. McCallum, and A. Peacock, "Blockchain technology in the energy sector: A systematic review of challenges and opportunities," *Renew. Sustain. Energy Rev.*, vol. 100, pp. 143–174, Feb. 2019.

[36] D. Efanov and P. Roschin, "The all-pervasiveness of the blockchain technology," *Procedia Comput. Sci.*, vol. 123, pp. 116–121, Jan. 2018.

[37] C. Machado and C. M. Westphall, "Blockchain incentivized data forwarding in MANETs: Strategies and challenges," *Ad Hoc Netw.*, vol. 110, Jan. 2021, Art. no. 102321.

[38] S. Hinojosa, D. Oliva, E. Cuevas, G. Pajares, O. Avalos, and J. Gálvez, "Improving multi-criterion optimization with chaos: A novel multi-objective chaotic crow search algorithm," *Neural Comput. Appl.*, vol. 29, no. 8, pp. 319–335, Apr. 2018.

[39] A. Chaudhuri and T. P. Sahu, "Feature selection using binary crow search algorithm with time varying flight length," *Expert Syst. Appl.*, vol. 168, Apr. 2021, Art. no. 114288.

[40] M. A. Mohamed, E. M. Awwad, A. M. El-Sherbeeny, E. A. Nasr, and Z. M. Ali, "Optimal scheduling of reconfigurable grids considering dynamic line rating constraint," *IET Gener., Transmiss. Distrib.*, vol. 14, no. 10, pp. 1862–1871, May 2020.

[41] M. A. Mohamed, H. M. Abdullah, A. S. Al-Sumaiti, M. A. El-Meligy, M. Sharaf, and A. T. Soliman, "Towards energy management negotiation between distributed AC/DC networks," *IEEE Access*, vol. 8, pp. 215438–215456, 2020.

[42] A. Agrawal, P. Farswan, V. Agrawal, D. C. Tiwari, and J. C. Bansal, "On the hybridization of spider monkey optimization and genetic algorithms," in *Proc. 6th Int. Conf. Soft Comput. Problem Solving*, Singapore: Springer, 2017, pp. 185–196.

[43] M. A. Mohamed, A. M. Eltamaly, and A. I. Alolah, "Sizing and techno-economic analysis of stand-alone hybrid photovoltaic/wind/diesel/battery power generation systems," *J. Renew. Sustain. Energy*, vol. 7, no. 6, Nov. 2015, Art. no. 063128.

[44] A. Gopal, M. M. Sultani, and J. C. Bansal, "On stability analysis of particle swarm optimization algorithm," *Arabian J. Sci. Eng.*, vol. 45, no. 4, pp. 2385–2394. 2020.

[45] M. A. Mohamed, A. M. Eltamaly, and A. I. Alolah, "PSO-based smart grid application for sizing and optimization of hybrid renewable energy systems," *PLoS ONE*, vol. 11, no. 8, Aug. 2016, Art. no. e0159702.

FENGYUAN YIN received the M.Sc. degree in control engineering, in 2019. Her research interests include electronic information technology, communication technology, and smart grid data processing.

ALI HAJJIAH received the B.Sc. degree in electrical engineering from Oklahoma State University, USA, in 1998, and the M.Sc. and Ph.D. degrees from Virginia Tech, USA, in 2003 and 2009 respectively. From 2011 to 2012, he was the Director of the Semiconductor Laboratory, Kuwait University. From January to August 2014, he joined IMEC Belgium as an Industrial Fellow working on enhancing the conversion efficiency of n-type PERT crystalline silicon solar cells. From 2015 to 2017, he was the Director of the Engineering Training and Alumni Center (ETAC), College of Engineering and Petroleum. He joined Virginia Polytechnic Institute and State University (Virginia Tech), USA, as a Visiting Scholar, in 2013, and subsequently the Catholic University of Leuven (KU Leuven), Belgium, in 2015 and 2017, respectively. He is currently full time as an Associate Professor with Kuwait University where he held key positions in the institute. He has been a member of several honor societies, such as The Golden Key National Honor Society, since 1995, the Tau Beta Pi Honor Society- Gamma Chapter, since 1997, the Eta Kappa Nu Honor Association —Omega Chapter, since 1997, and finally the Phi Sigma Theta National Honor Society, since 2002. His research interests include processing and fabrication of Si and III-V semiconductor lasers and thin film solar cells. He is also working on efficiency improvement and device physics of Perovskite/Si tandem solar cells.

KITTISAK JERMSITTIPARSERT received the Ph.D. degree in social sciences from Kasetsart University, Thailand. He is currently a Researcher with the Chulalongkorn University Social Research Institute. He is also a part-time Researcher with Ton Duc Thang University, and the Secretary General of the Political Science Association, Kasetsart University. His areas of expertise are politics, public policy, business, development, and energy management.

AMEENA SAAD AL-SUMAITI (Senior Member, IEEE) received the B.Sc. degree in electrical engineering from United Arab Emirates University, United Arab Emirates, in 2008, and the M.Sc. and Ph.D. degrees in electrical and computer engineering from the University of Waterloo, Canada, in 2010 and 2015, respectively. She was a Visiting Assistant Professor with MIT, Cambridge, MA, USA, in 2017. She is currently an Assistant Professor with the Department of Electrical and Computer Engineering, Khalifa University, Abu Dhabi, United Arab Emirates. Her research interests include intelligent systems, energy economics, and energy policy.

SALAH K. ELSAYED received the B.Sc. (Hons.) and M.Sc. degrees in electrical engineering from the Electrical Engineering Department, Faculty of Engineering, Al-Azhar University, Cairo, Egypt, in 2005 and 2009, respectively, and the Ph.D. degree from the Department of Electrical Engineering, University of Al-Azhar, in 2012. From 2012 to 2017, he was a Lecturer with the Electrical Engineering Department AL-Azhar University, then he promoted to an Associate Professor, in 2017. He joined the Electrical Engineering Department, Faculty of Engineering, Taif University, Saudi Arabia. His research interests include power systems analysis and operation, power systems stability and control, power system optimization techniques, artificial intelligence systems applications in power systems, and renewable energy sources.

SHERIF S. M. GHONEIM (Senior Member, IEEE) received the B.Sc. and M.Sc. degrees from the Faculty of Engineering at Shoubra, Zagazig University, Egypt, in 1994 and 2000, respectively, and the Ph.D. degree in electrical power and machines from the Faculty of Engineering, Cairo University, in 2008. Since 1996, he has been teaching with the Faculty of Industrial Education, Suez Canal University, Egypt. From 2005 to 2007, he was a Guest Researcher with the Institute of Energy Transport and Storage (ETS), University of Duisburg-Essen, Germany. He joined the Electrical Engineering Department, Faculty of Engineering, Taif University, as an Associate Professor. His research interests include grounding systems, dissolved gas analysis, breakdown in SF6 gas, and AI technique applications.

MOHAMED A. MOHAMED (Member, IEEE) received the B.Sc. and M.Sc. degrees in electrical engineering from Minia University, Minia, Egypt, in 2006 and 2010, respectively, and the Ph.D. degree in electrical engineering from King Saud University, Riyadh, Saudi Arabia, in 2016. Since 2008, he has been a Faculty Member with the Department of Electrical Engineering, College of Engineering, Minia University. He joined the College of Electrical Engineering and Automation, Fuzhou University, China, as a Postdoctoral Research Fellow, in 2018. He has supervised multiple M.Sc. and Ph.D. theses, worked on a number of technical projects. He has published various articles and books. His research interests include power system analysis, renewable energy integration, energy management, power electronics, electrical vehicles, optimization, smart islands, smart cities, and smart grids. He has also joined the editorial board of some scientific journals and the steering committees of many international conferences.